Excitation of the $4\,^3S$ and $3\,^3P$ Levels of Helium by Electron Impact*

R. J. Anderson, R. H. Hughes, J. H. Tung, and S. T. Chen
Department of Physics, University of Arkansas, Fayetteville, Arkansas 72701
(Received 26 February 1973)

The exchange excitation of the $4\,^3S$ and $3\,^3P$ levels of helium by electron impact has been studied by means of time-resolved spectroscopy of the $4\,^3S \rightarrow 2\,^3P$ ($\lambda = 4713$-Å) and $3\,^3P \rightarrow 2\,^3S$ ($\lambda = 3889$-Å) transitions. Measurements were carried out for incident electron energies in the range 50–400 eV at helium-gas pressures of 8 and 4 mtorr. Radiative cascade transitions from the $n\,^3P$ levels and from the $n\,^3S$ and $n\,^3D$ levels contributed 12 and 10% to the total $4\,^3S$ and $3\,^3P$ populations, respectively, at 50 eV. These fractions increased to about 30 and 40%, respectively, at 400-eV electron-impact energy. The $4\,^3S$ and $3\,^3P$ direct-excitation cross sections were observed to decrease with increasing electron impact according to the relation $(\text{energy})^{-3}$. This result is in agreement with the theoretical predictions of Ochkur and Bratsev.

I. INTRODUCTION

Many experimenters have used the optical method to examine the phenomenon of electron-exchange excitation in electron-atom collisions. Particular emphasis has been given to the study of the triplet levels of the He I spectrum since they can be directly excited only through the exchange mechanism. Absolute measurements of the direct-excitation cross section and its dependence upon incident-electron energy have been obtained for several of the He I triplet levels. However, discrepancies presently exist between many of these measurements and the corresponding theoretical predictions. One example is the apparent discrepancy between theory and experiment in predicting the relative energy dependence exhibited by the direct-excitation cross-section curve (excitation function).

In the case of helium the Born-Oppenheimer theory predicts that triplet-state excitation functions will have a peak just above the threshold energy and then experience a rapid monotonic decrease with increasing energy of the incident electron. This rate of decrease of the direct cross section with electron energy E is calculated to be E^{-2}, E^{-3}, and E^{-4} for the ^3S, ^3P, and ^3D levels, respectively.[1] Calculations of the direct-excitation cross section carried out using the expansion technique of Ochkur and Bratsev predict a E^{-3} dependence for all of the triplet-level cross sections.[2] Previous experimental studies of this energy dependence have produced contradictory results.[3] The theoretical calculations become more valid at the higher energies (above 100 eV). However, this is a difficult region to interpret experimental results because secondary excitation mechanisms, such as radiative cascade, generally make significant contributions to the low-level optical measurements. The $4\,^3S$, $3\,^3P$, and $3\,^3D$ apparent-cross-section energy dependence determined by Kay and Showalter[4] indicates a single E^{-3} dependence for the $4\,^3S$ cross section for the higher energies. However, they found that the $3\,^3P$ and $3\,^3D$ levels have excitation functions which exhibit a far more complicated energy dependence at these higher energies. A log-log plot of their apparent cross section versus incident-electron energy shows that the $3\,^3P$- and $3\,^3D$-level excitations each exhibit a E^{-1} dependence for energies above approximately 100 eV. Subtracting this energy dependence from the original data points leaves a second component that varies as $E^{-3.5}$ and $E^{-3.7}$ for the $3\,^3P$ and $3\,^3D$, respectively. The slow components are attributed by the authors of Ref. 4 to the effects of secondary excitation on the levels in question.

The present work uses time-resolved spectroscopy to determine the energy dependence of the direct-excitation cross section. The effects of secondary excitation mechanisms which have temporal decay rates different from the radiative rate of the upper level of the transition under study are subtracted off from the total light intensity. This technique provides direct information about the excited-atom density produced by direct electron-impact excitation. The time-resolved technique is a simple and useful method to isolate, identify, and quantitively measure the effects of secondary excitation mechanisms and therefore can be used effectively in conjunction with absolute-intensity measurements to determine direct-excitation cross sections.

II. EXPERIMENT

The time-resolving apparatus shown in Fig. 1 was similar to that used in our previous experiments.[5] Helium gas passed through a cooled trap and into the excitation chamber through a small orifice. The rate of helium-gas flow was held

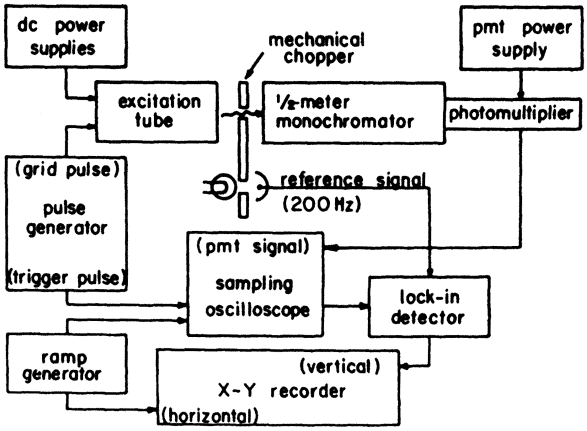

FIG. 1. Block diagram of the experimental apparatus.

constant by means of a precision gas-metering valve. A cooled zeolite molecular sieve trap was connected to the excitation chamber to remove impurity gases produced during the experiment. The target-gas pressure was continuously monitored by means of calibrated ion and Pirani gauges.

The time-resolved apparatus employed a gated electron beam as the excitation mechanism. The electron source was an electron gun removed from a 6EM5 radio tube. The gun was initially biased to cutoff by applying a negative dc potential to the control grid and then biased to conduct by applying to the grid a positive variable-width pulse. The pulse width and pulse repetition rate used in the present experiment were 600 ns, and 50 kHz, respectively. It was observed experimentally that the length of the electron beam pulse was sufficient to allow equilibrium of the excited-state population. (The light intensity reached a constant value before beam cutoff.) The pulsed electron beam passed through a field-free collision region and was collected in a deep Faraday cup. The grid structure of the excitation tube and the Faraday cup were modified to reduce the influence of slow and secondary electrons upon the excitation process. (A grid with a retarding potential was placed adjacent to the collision-chamber entrance and spiraled aluminum foil was inserted into the rear of the Faraday cup.)

The collisionally induced radiation left the collision chamber at right angles to the electron beam and was focused with unit magnification along the slits of a 0.5-m–focal-length monochromator operated at a spectral slit width of $\Delta\lambda = 8$ Å. The photodetection system employed a sampling oscilloscope to analyze the decay of the collisional radiation. The signal-to-noise capabilities of the sampling system were increased by use of a double-modulation scheme employing a lock-in detection system.[6] The resulting x-y trace of the time-resolved system was a plot of light intensity versus time. Absolute calibration of the time axis was achieved by monitoring a signal of known frequency with the sampling system.

Relative measurements of the apparent cross section were obtained using the time-resolved system operated in a dc mode. The 200-Hz lock-in detection system was used to detect the collisional radiation. The image of the electron beam was focused with unit magnification horizontally across the monochromator slit openings. Measurements of the integrated light intensity were taken at several values of incident-electron energy. The monochromator wavelength was scanned over the spectral line, producing a record of the line profile and background spectra. The helium-gas pressure was held constant during the measurements, and the electron beam current collected in the Faraday cup was monitored. Small traces of impurity gases were observed to be present in the excitation chamber. The principal impurity was nitrogen, which has strong bands lying near the $\lambda = 3889$ Å and $\lambda = 4713$ Å helium lines under investigation. The presence of nitrogen did not interfere with the intensity measurements of the $\lambda = 3889$ Å line, since this is a strong helium line and the $\Delta\lambda = 8$ Å spectral slit width of the monochromator effectively isolated it from the $\lambda = 3914$ Å band of the nitrogen spectrum. However, it was not possible to spectrally resolve the $\lambda = 4709$ Å nitrogen band from the $\lambda = 4713$ Å helium line. The $\lambda = 4713$ Å signal contained less than 5% nitrogen contamination at 50 eV and approximately 25% at 300 eV. The nitrogen background signal could be determined from the spectral intensity versus wavelength profile since the narrow helium line rode on top of the broader nitrogen band. An additional correction was carried out for the $3\,^3P - 2\,^3S$ ($\lambda = 3889$ Å) transition. Below approximately 100 eV, the $\lambda = 3889$ Å line is subject to polarization effects. The polarization measurements of Hughes *et al.*[7] were used to correct for the effects of the $3\,^3P$ anisotropic radiation pattern and the polarization-sensitive response of the detection system. This procedure yielded a multiplicative polarization-correction factor which varied from 0.91 at 50 eV to 1.00 at 250 eV incident-electron energy.

III. TREATMENT OF DATA

The excitation pulse was an electron beam which established excitation equilibrium before it was turned off at time $t = 0$. In the simple case of two excited states j and k, where state k cascades into state j, the population-rate equation of state j at time $t > 0$ is given by

$$\dot{n}_j = n_k^0 A_{kj} e^{-t/\tau_k} - n_j/\tau_j , \quad (1)$$

where n_j is the density of atoms in state j, n_k^0 is the density of atoms in state k at $t=0$, A_{kj} is the transition probability $k \rightarrow j$, and τ_k and τ_j are the lifetimes of the states k and j, respectively.

The population of state j as a function of time after the cessation of electron excitation is given by the solution of Eq. (1), which is

$$n_j = \beta e^{-t/\tau_j} + \gamma_k e^{-t/\tau_k} , \quad (2)$$

where

$$\beta = n_j - \gamma_k , \quad \gamma_k = n_k^0 A_{kj} \tau_j (1 - \tau_j/\tau_k)^{-1} ,$$

and n_j^0 is the total density of atoms in state j at time $t=0$. Also, at $t=0$, $n_j^0 = n_j^* + \tau_j n_k^0 A_{kj}$. Therefore, $n_j^* = \beta + \gamma_k \tau_j/\tau_k$, where n_j^* is the number density of atoms excited by direct excitation.

The apparent cross section for populating state j by all available means is the one normally measured in a dc electron-beam experiment. It is written as $Q_j' = n_j^0 (\Phi \rho \tau_j)^{-1}$, where Φ is the electron flux and ρ the atom number density. The direct-excitation cross section can be defined in a similar manner and is defined as $Q_j = n_j^* (\Phi \rho \tau_j)^{-1}$. Cross sections for excitation to higher levels are defined in an analogous manner. In the absence of secondary excitation mechanisms (e.g., radiative cascade) the two cross sections are equal.

If $\tau_k > \tau_j$, then a semilog plot of n_j vs t [Eq. (2)] will show two characteristic decay modes having positive initial intercepts β and γ_k. If we define $f_\beta = \beta/n_j^0$ and $f_k = \gamma_k/n_j^0$, which are the fractions of the total decay having intercepts β and γ_k, respectively, then $f_\beta + f_k = 1$. In the present case state k represents several cascading levels whose individual lifetimes cannot be resolved by the present apparatus. They are therefore observed as a single long-lived decay mode with a composite decay constant τ_k. The direct-excitation cross section is our primary interest. It can be expressed in terms of experimentally measurable quantities as

$$Q_j = Q_j' (f_\beta + f_k \tau_j/\tau_k) . \quad (3)$$

Errors in the determination of Q_j occur if $\tau_k \simeq \tau_j$ such that these decays cannot be resolved as separate decays. The fraction f_β then includes the cascade from k as well as direct excitation to j. Under most circumstances this occurs when $\tau_k < 2\tau_j$ in the present apparatus. This difficulty does not arise in the cascade analysis of the $4\,^3S$ level since the cascading $n\,^3P$ levels ($n=4,5,\ldots$) have lifetimes which are more than twice that of the $4\,^3S$ level. (Gabriel and Heddle[8] report theoretical lifetimes of 150 and 260 ns for the $5\,^3P$ and $6\,^3P$ levels as compared to 64 for the $4\,^3S$ level.) However, this problem arises during the cascade analysis of the $3\,^3P$ level, where several cascading $n\,^3S$ and $n\,^3D$ levels have lifetimes that cannot be experimentally resolved from the natural $3\,^3P$ decay.

Examination of the theoretical lifetimes reported in Ref. 8 shows that the $n\,^3S$ levels have lifetimes of 64, 110, and 180 ns for $n=4, 5$, and 6, respectively, and that the $n\,^3D$ levels have lifetimes of 60, 108, and 146 ns for $n=5, 6$, and 7, respectively. The lifetime of the $3\,^3P$ level is reported by the same source to be 97 ns. All of these lifetime values fall within the resolution limit of our apparatus, which implies a possible cascade contribution to f_β for the $3\,^3P$ level. Fortunately, an upper limit of the nondirect cascade contribution to f_β can be estimated.

The apparent cross section $Q'(3\,^3P)$ is proportional to the total $3\,^3P$ population produced by all means, and the cross section $Q(3\,^3P)$ represents direct excitation. Let $Q'(3\,^3P) = Q(3\,^3P) + \sum_k Q(k \rightarrow 3\,^3P)$. The cross section $\sum_k Q(k \rightarrow 3\,^3P)$ represents the cascade contribution to the apparent cross section $Q'(3\,^3P)$. The ratio $Q(k \rightarrow 3\,^3P)/Q'(3\,^3P)$ is the fraction of the total $3\,^3P$ population produced by cascade transitions from the upper k state. Estimates of the cross sections for the cascading levels which cannot be resolved from the $3\,^3P$ natural decay can be obtained from the expressions

$$Q(n\,^3S \rightarrow 3\,^3P) = \frac{Q'(n\,^3S) A(n\,^3S \rightarrow 3\,^3P)}{A(n\,^3S)} ,$$

$$Q(n\,^3D \rightarrow 3\,^3P) = \frac{Q'(n\,^3D) A(n\,^3D \rightarrow 3\,^3P)}{A(n\,^3D)} ,$$

where $n=4, 5$, and 6 and $n=5, 6$, and 7 for the ^3S and ^3D levels, respectively. The absolute apparent-cross-section data of St. John *et al.*[9] and the theoretical transition probabilities reported in Ref. 8 were used to evaluate the fraction of the $3\,^3P$ population which could not be resolved from the direct $3\,^3P$ excitation. (Apparent cross sections for the $6\,^3S$ and the $7\,^3D$ levels were not reported by St. John *et al.* These cross sections were estimated assuming a n^{-3} cross-section dependence.) The cascade contributions, $n\,^3S \rightarrow 3\,^3P$, were estimated to be 9%, 2%, and less than 1% for the $n=4, 5$, and 6 levels, respectively, at 100-eV incident-electron energy. At this electron energy, the total $n\,^3D$ contribution ($n=5,6$, and 7) is estimated to be approximately 2%. A total of approximately 13% is estimated to be the fraction of the $3\,^3P$ population produced by cascade transitions which cannot be resolved from the natural $3\,^3P$ decay. This represents an upper limit of the cascade contribution to f_β. The present $3\,^3P$ lifetime measurement (101 ±5 ns) ex-

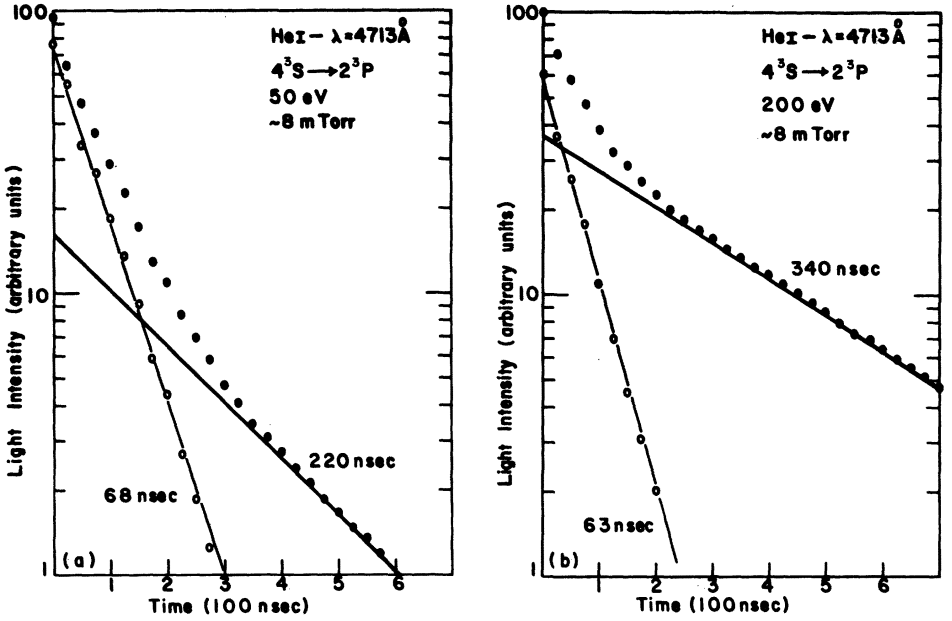

FIG. 2. Example of the λ =4713 Å decay curve taken at 8-mtorr gas pressure and at (a) 50-eV and (b) 200-eV electron-impact energy. The long-lived decay mode represents the composite decay of several higher n^3P states into the $4\,^3S$ level. The short-lived decay is identified as the direct-excitation contribution to the $4\,^3S$ population.

hibits reasonable agreement with the measurements of other experimenters[10] and suggests that our analysis of the situation is proper. No cascade corrections are applied to the cross sections presented in this paper. The omission of these corrections leads to small overestimation of the true $3\,^3P$ cross section and has a negligible effect on the $4\,^3S$ cross section.

IV. RESULTS AND DISCUSSION

The intensity of the collisional radiation was monitored, using time-resolved techniques, for incident-electron energies between 50 and 400 eV and at helium-gas pressures of 4 and 8 mtorr. Several intensity decay curves were obtained at each electron energy and an average curve was plotted on semilog graph paper. Typical decay curves for the $4\,^3S \rightarrow 2\,^3P$ and $3\,^3P \rightarrow 2\,^3S$ transitions are shown in Figs. 2 and 3. The contribution of direct excitation to the total light intensity was separated from that of the cascade transitions by subtracting the long-lived cascade component from the original data points. The decay constant of each mode was measured and the direct-excitation contribution was identified through comparison

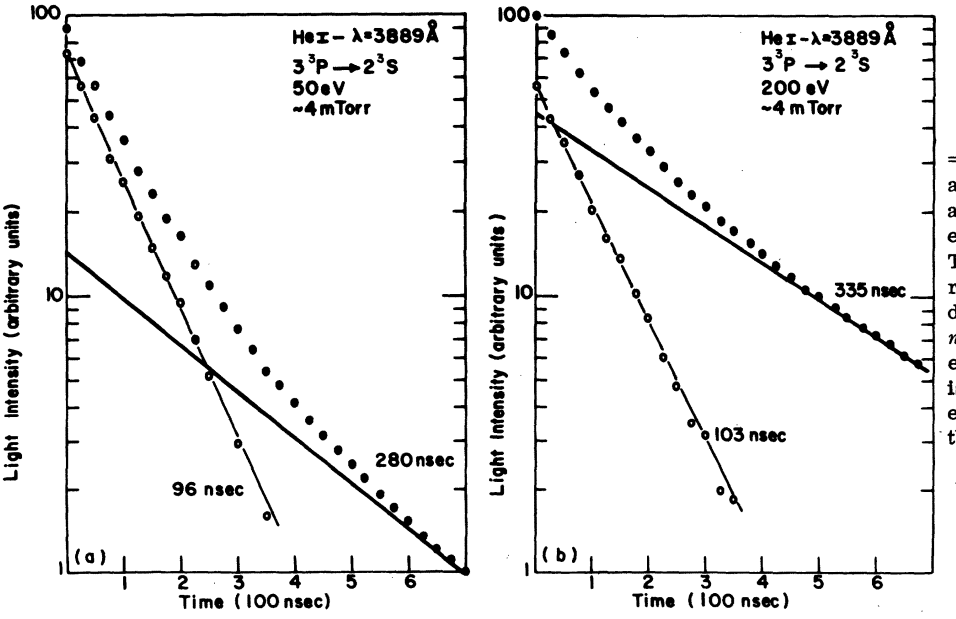

FIG. 3. Example of the λ =3889 Å decay curve taken at 4-mtorr gas pressure and at (a) 50-eV and (b) 200-eV electron-impact energy. The long-lived decay mode represents the composite decay of several n^3S and n^3D states into the $3\,^3P$ level. The short-lived decay is identified as the direct-excitation contribution to the $3\,^3P$ population.

TABLE I. Estimates of cross sections for $4\,^3S$ direct electron impact in units of 10^{-20} cm^2. Listed uncertainties are relative to the experimental measurements of this paper only and primarily reflect reproducibility uncertainties.

Energy (eV)	τ_j (ns)	τ_k (ns)	f_β (%)	f_k (%)	$f_\beta + f_k\tau_j/\tau_k$ (%)	$Q'(4\,^3S)$ (10^{-20} cm^2)	$Q(4\,^3S)$ (10^{-20} cm^2)
50	66	222	82	18	88	27.2	23.8 ± 3.3
55	71	231	81	19	87	18.7	16.2 ± 2.0
80	66	248	80	20	86	5.9	5.1 ± 0.5
100	69	252	72	29	80	3.3	2.6 ± 0.2
120	61	258	69	31	76	2.1	1.6 ± 0.2
150	64	314	62	38	70	1.1	0.7 ± 0.1
170	64	288	59	41	68	0.8	0.5 ± 0.1
200	63	364	64	36	71	0.5	0.4 ± 0.1
250	67	380	62	38	69	0.3	0.2 ± 0.1
300	64	383	63	37	69	0.2	0.1 ± 0.03

with the corresponding theoretical transition probabilities for the $4\,^3S$ and $3\,^3P$ levels. The short-lived decay modes have lifetimes of approximately 66 ± 5 and 101 ± 5 ns for the $\lambda = 4713$ Å and $\lambda = 3889$ Å transitions, respectively. These values are in good agreement with the corresponding theoretical values of 63.8 and 96.6 ns reported by Gabriel and Heddle.[8] The long-lived decay mode has a lifetime which appears to increase with increasing electron energy and cannot be identified with the lifetime of any one particular higher-energy level. It appears rather to be the composite result of multiple cascade transitions.

Apparent-cross-section measurements for the $4\,^3S$ and $3\,^3P$ levels were carried out using a dc electron beam at electron energies corresponding to those of the time-resolved measurements. The dc measurements were obtained at several helium-gas pressures and electron beam currents. Extrapolation of these data was used to obtain apparent cross sections which were independent of pressure and current effects. When necessary the measurements were corrected for effects of polarization and impurity gases. The corrected $4\,^3S$ and $3\,^3P$ apparent cross sections were placed on an absolute scale by normalizing to the absolute cross sections at 100 eV reported by St. John *et al.*[9] (Our apparent-excitation functions had shapes similar to those reported in Ref. 9 for energies below 100 eV.)

The experimentally determined values of f_β, f_k, and Q_j' for the $4\,^3S$ and $3\,^3P$ levels, listed in Tables I and II, respectively, were substituted into Eq. (3) to obtain estimates of the absolute

TABLE II. Estimates of cross sections for $3\,^3P$ direct electron-impact excitation in units of 10^{-20} cm^2. Listed uncertainties are relative to the experimental measurements of this paper only. They primarily reflect reproducibility uncertainties and do not reflect a possible overestimate due to incomplete resolution (see text).

Energy (eV)	τ_j (ns)	τ_k (ns)	f_β (%)	f_k (%)	$f_\beta + f_k\tau_j/\tau_k$ (%)	$Q'(3\,^3P)$ (10^{-20} cm^2)	$Q(3\,^3P)$ (10^{-20} cm^2)
50	96	282	85	15	90	111.0	99.9 ± 1.1
60	96	278	90	10	94	69.6	65.4 ± 7.8
80	101	278	80	20	87	29.5	25.6 ± 3.1
100	101	282	72	28	82	15.3	12.6 ± 1.3
120	103	296	70	30	80	9.1	7.3 ± 1.2
150	105	306	60	40	74	5.2	3.9 ± 0.8
170	101	316	59	41	72	3.8	2.8 ± 0.6
200	103	335	55	45	69	2.4	1.7 ± 0.4
250	101	335	55	45	69	1.7	1.2 ± 0.3
300	101	354	50	50	64	1.2	0.8 ± 0.2
400	101	364	45	55	62	0.5	0.3 ± 0.1

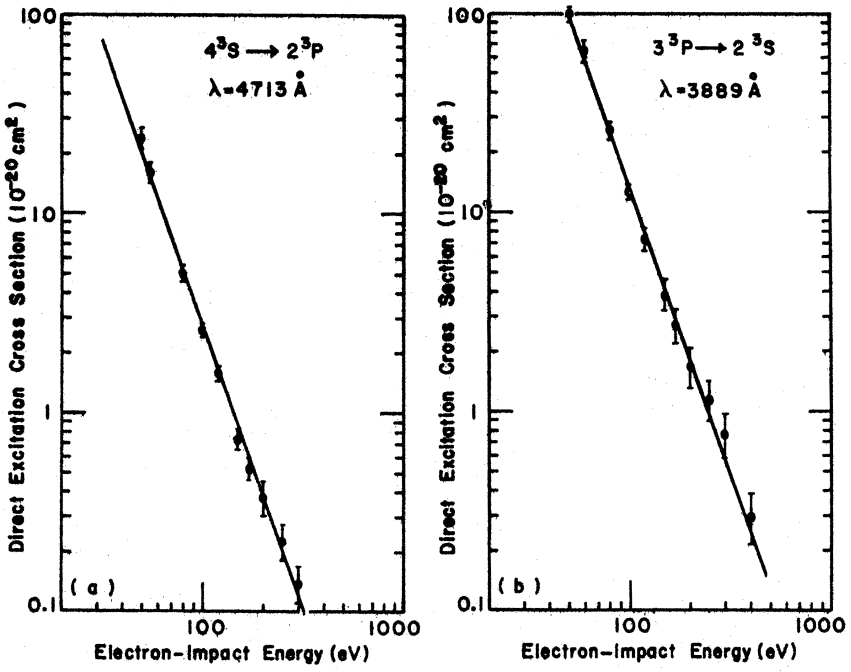

FIG. 4. Direct-excitation cross section vs electron-impact energy at zero effective pressure with corrections for polarization and nitrogen-gas impurities. (a) $4\,^3S$ level: The direct-excitation cross section decreases with increasing incident-electron energy with a slope of −2.8 ± 0.2. (b) $3\,^3P$ level: The direct-excitation cross section decreases with increasing incident-electron energy with a slope of −3.0 ± 0.2.

values of the corresponding direct-excitation cross sections. The uncertainties associated with the absolute cross sections listed in Tables I and II are relative to the experimental measurements of this paper only. They do not take into account possible uncertainties in the data of Ref. 9, which were used to place our relative measurements on an absolute scale.

The relative values of the $4\,^3S$ and $3\,^3P$ direct-excitation cross sections are plotted on a log-log scale as a function of electron-impact energy (Fig. 4). The error bars represent the limits of experimental reproducibility and take into account measurement errors present in each of the quantities used to determine the direct cross section. A weighted least-squares analysis of the data indicates that the $4\,^3S$ direct cross section decreases with increasing electron energy according to the relation $(\text{energy})^{-2.8\pm0.2}$, while the $3\,^3P$ cross section decreases as $(\text{energy})^{-3.0\pm0.2}$. In each case the rate of decrease exhibits reasonable agreement with the dc intensity measurements of Kay and Showalter.[4]

It appears that above electron energies of 50 eV both the $4\,^3S$ and $3\,^3P$ direct cross sections follow an $(\text{energy})^{-3}$ dependence. This result would appear to contradict the $(\text{energy})^{-2}$ dependence predicted by Born-Oppenheimer theory for the $4\,^3S$ level, and instead tends to support the expansion technique of Ochkur and Bratsev. The present work demonstrates the versatility and promise of time-resolved spectroscopy as a research tool when used in conjunction with absolute-intensity measurements.

*Supported in part by the National Science Foundation.

[1]N. F. Mott and H. S. W. Massey, *The Theory of Atomic Collisions*, 3rd ed. (Claredon, Oxford, England, 1965).
[2]V. I. Ochkur and V. F. Bratsev, Opt. Spektrosk. **19**, 490 (1965) [Opt. Spectrosc. **19**, 274 (1965)].
[3]B. L. Moiseweitsch and S. J. Smith, Rev. Mod. Phys. **40**, 246 (1968).
[4]R. B. Kay and J. G. Showalter, Phys. Rev. A **3**, 1998 (1971).
[5]R. J. Anderson, R. H. Hughes, and T. G. Norton, Phys. Rev. **181**, 198 (1969).
[6]R. J. Anderson and R. H. Hughes, Phys. Rev. A **5**, 1194 (1972).
[7]R. H. Hughes, R. B. Kay, and L. D. Weaver, Phys. Rev. **129**, 1630 (1963).
[8]A. H. Gabriel and D. W. O. Heddle, Proc. R. Soc. Lond. A258, 124 (1960).
[9]R. M. St. John, F. L. Miller, and C. C. Lin, Phys. Rev. **134**, A888 (1964).
[10]W. R. Pendleton and R. H. Hughes, Phys. Rev. **138**, A683 (1965).

PHYSICAL REVIEW A VOLUME 8, NUMBER 2 AUGUST 1973

Time and Pressure Dependence of the Vacuum-Ultraviolet Radiation in Neon

Peter K. Leichner
Department of Physics and Astronomy, University of Kentucky, Lexington, Kentucky 40506
(Received 6 March 1973)

A 250-keV electron accelerator was used to carry out time-dependent studies in neon gas at the wavelength of the $^1P_1$ and $^3P_1$ resonance line and the 850-Å continuum over a wide range of pressures, up to 1000 Torr. The resonance line decays exponentially with a lifetime that is governed predominantly by the escape of resonance radiation to the walls of the emission chamber and by three-body destruction of the resonance states. The main continuum near 859 Å comes to a maximum well after termination of the excitation pulse and then decays with a lifetime that is very long at low pressures. However, this lifetime decreases with increasing pressure at low and intermediate pressures and assumes a nearly constant value of 5.1 μsec at the highest pressures. From the time-dependent studies it is proposed that both $^1P_1$ and $^3P_1$ resonance states are converted to metastable molecular states by three-body collisions. The metastable molecules in turn may undergo two- and three-body collisions with ground-state atoms which convert them to radiative molecules that radiate the 850-Å continuum with a lifetime of about 5.1 μsec.

I. INTRODUCTION

Recent investigations of the vacuum-ultraviolet (vuv) radiation in argon[1] and helium[2] have shown that the excitation of noble gases by energetic charged particles provides a valuable tool for measuring the time and pressure dependence of the resonance radiation and continuous emission in these gases. The objective of this paper is to report lifetime measurements of the 740-Å resonance line and the 850-Å continuum in pure neon gas over wide pressure ranges.